Assessment of the Road Surface Condition with Longitudinal Acceleration Signal of the Car Body

Krzysztof Prażnowski [1,*], Jarosław Mamala [1], Michał Śmieja [2] and Mariusz Kupina [3]

[1]   Department of Vehicle, Faculty of Mechanical Engineering, Opole University of Technology,
     45-271 Opole, Poland; j.mamala@po.edu.pl
[2]   Faculty of Technical Sciences, University of Warmia and Mazury in Olsztyn, 10-710 Olsztyn, Poland;
     smieja@uwm.edu.pl
[3]   Department of Mechanics and Structural Engineering, Faculty of Civil Engineering and Architecture,
     Opole University of Technology, 45-061 Opole, Poland; m.kupina@po.edu.pl
*   Correspondence: k.praznowski@po.edu.pl; Tel.: +48-77-449-8443

Abstract: On the basis of road tests, the authors assessed the feasibility of the vehicle body acceleration values for the purposes of assessing road surface characteristics in terms of its roughness. Short-term Fourier Transform (STFT) was used for the analysis of the recorded signal. The spectra obtained in successive frequency bands demonstrate the amplitudes originating from the natural vibrations of the rolling wheel and forces resulting from the interaction with the road roughness. The article focuses on the relationships between the road roughness and the ratios of individual amplitudes in a specific frequency band of the vehicle body acceleration values. Amplitude values derived on the basis of successive windows were averaged for analogous, arbitrarily assumed local frequency bands. The value characterizing the road surface condition provided the information regarding the mean amplitude value in specific frequency ranges depending on the instantaneous velocity of the car body and the condition of the road surface on which it was moving. In cases where the road was free of any visible roughness, the obtained mean amplitude value in the analyzed spectrum window, for the adopted vehicle velocity range from 50 km h to 100 km/h, did not exceed 0.02 m/s^2. It was also demonstrated that the road surface roughness leads to an increase in the mean amplitude value from 0.07 m/s^2 to 0.16 m/s^2.

Keywords: road surface; vehicle vibration; pavements classification

1. Introduction

Acceleration measurement systems are used in many fields of science, such as mechanical engineering, construction and medicine. The developed systems are aimed at determining the inputs acting on the tested object through locometric measurements, such as speed or acceleration. Karacocuk et al. [1] proposed a system that is able to detect an athlete's respiratory rate using inertial sensors such as gyroscopes and accelerometers. Seyedfakhreddin and Sharmistha [2] used the fusion method to estimate cardiopulmonary parameters from a photoplethysmography (PPG) signal and an accelerometer, which significantly reduces motion artifacts from PPG signals.

The unevenness in the structure of the road surface cause changes in the value and direction of the resultant force acting on a rolling wheel. The consequence is the vibration of the car body [3,4]. The authors of [3] presented the results of research on the identification of directional distribution of vibrations transmitted to the vehicle body. The results showed that the pattern of the occurring vibrations is diversified in terms of directional axes and location of their occurrence in the vehicle structure.

Another study [5], discusses the unified theory of dynamics of vehicle–pavement interaction under stochastic load. When a vehicle drives at the speed of about 40 km/h, the oscillations of the vehicle's sprung and unsprung masses are insignificant (reaching 5.2 Hz), which correlates with road roughness [6]. Stochastic driving of the wheel over the road defects (e.g., depressions, potholes, bumps, ruts, etc.) has a significant impact on it. This results in changes to the suspension deflection, resulting in the longitudinal and transverse body roll angles of the vehicle chassis [7,8]. As a result, the linear acceleration components of the body are generated. Due to the shape of the profile of the road surface roughness, differences in the determined (e.g., sinusoidal) and random profiles occur [9]. For their geometric analysis and identification, the power spectral density function, the amplitude spectrum and statistical parameters are used. In the article [10], the authors made a comparative analysis of longitudinal road profiles between the old and new surface. As a result of the analysis, some disadvantages of the international roughness index (IRI) were presented as well as advantages of the spectral power density (PSD) of road irregularities to reflect the road profile. The authors of the study [11,12] paid special attention to the observation of vibration magnitude for resonance bands of sprung and unsprung masses. In the paper [12] They used the TFR (time–frequency representation) method to analyze the car suspension vibration signal to observe and evaluate the vibrations. The road irregularity is considered a Gaussian random process and is modelled by means of a simple exponential PSD. Another article [13] described the measurement of radial directional natural frequency and the damping ratio in a vehicle tire has also been studied. The results show that experimental conditions can be considered as the parameters that shift the natural frequency and damping ratio.

Due to the shape of uneven road surface, described as the sum of sinusoidal waves of different amplitudes and frequency ranges [14]. The authors in the article described a system using a smartphone accelerometer to record vehicle vibrations, in which the Z-axis reading corresponds to vertical vibrations of the vehicle. According to the ISO 8606 standard of 1995, road surfaces were divided into eight classes, for which the (PSD) function was used, which are marked with letters: A, B, C, D, E, F, G, H (Figure 1).
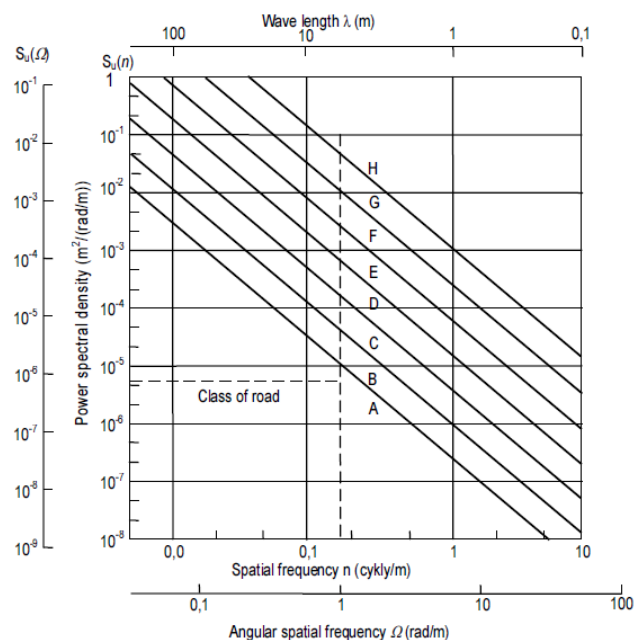
Figure 1. The center values of spectral density of unevenness according to ISO 8606 [15].

Materials and methods should be developed with sufficient details to allow others to replicate and build on the published results. The road profile described by the PSD function refers to the waves W

(rad/m), where $\Omega_0 = 1$ (rad/m) is the reference wave (formula1). Each class is defined by the reference value $S_u(\Omega_0)$ whose values are shown in Table 1.

$$S_u(\Omega) = S_u(\Omega_0) \cdot \left(\frac{\Omega}{\Omega_0}\right)^{-k}, \tag{1}$$

Table 1. Classification of pavements according to Road unevenness [15].

Class	$S_u(\Omega_0)(m^2/(rad/m))$ at $\Omega_0 = 1$ rad/m		
	Lower Bound	Geometric Average	Upper Bound
A	-	1×10^{-6}	2×10^{-6}
B	2×10^{-6}	4×10^{-6}	8×10^{-6}
C	8×10^{-6}	16×10^{-6}	32×10^{-6}
D	32×10^{-6}	64×10^{-6}	128×10^{-6}
E	128×10^{-6}	256×10^{-6}	512×10^{-6}
F	512×10^{-6}	1024×10^{-6}	2084×10^{-6}
G	2084×10^{-6}	4096×10^{-6}	8192×10^{-6}
H	8192×10^{-6}	$16,384 \times 10^{-6}$	-

The letter A indicates the road with the best road surface quality, while the letter H indicates the road with the worst quality. The presented classes of spectral density of road unevenness refer to the known wavelength of road unevenness.

1.1. State of the Art

Many research centers have focused their research on developing new and improving existing methods of collecting information on road surface condition. In paper [16], the authors presented a review of literature on the distress and related detection methods. Chiculita and Frangu [17] developed and studied configuring the accelerometer to measure vehicle vibration in off-line mode. According to their authors, it is supposed to be an alternative to large and expensive measurement systems. Katicha, El Khoury and Flintsch [18] proposed a model for a probing the vehicle, based on the quarter car model in which the Probe Vehicle Roughness Index (PVRI) was calculated. The PVRI, which is similar to the International Roughness Index (IRI), refers to the whole car (not a quarter of the car).

In the paper [19], the authors investigated the possibility of using a cheap and easy to use Android smartphone to estimate road irregularities and traffic volume. The authors determined that the acceleration data from the smartphone has a linear dependence on road unevenness partially dependent on speed. The exploration algorithm is based on the Gaussian model. The article [20] proposes a method of measuring the roughness of the surface of paths for pedestrians and cyclists based on the global positioning system (GPS) and accelerometer sensors in bicycle smartphones. The article [21] presents the technique of detection and crowdsourcing with the use of a smartphone to detect the condition of the road surface, the aim of which was to improve the classification accuracy of road surface condition detection using DTW (dynamic time warping). It was determined that DTW shows high accuracy and performance due to the possibility of comparing two time-dependent series of data, which may vary in speed. In the paper [22] Du et al. described the method of recognizing road surface damage using a smartphone acceleration sensor. The Gauss background model is optimized by an inference system based on fuzzy logic. They showed that the accuracy of road surface damage recognition was 96.03%.

The vertical linear vibrations of the body of a moving vehicle are then used to assess the condition of the road surface. These systems have the potential to provide the data necessary to estimate the road

surface unevenness, i.e., the international roughness index (IRI) [21,23]. To determine the IRI value, the value of vertical displacement (resulting from pits, bumps and humps on the road) is used [24]. The IRI is then calculated by an indirect method using a mathematical model called the "quarter car".

The most commonly recommended units are meters per kilometer (m/km) or millimeters per meter (mm/m) [25]. In the paper [10], however, it was pointed out that a description of the road profile with a correlation to the vehicle and human body vibration response stronger than the IRI would be more appropriate, due to the time of exposure of vehicle vibrations to the human body. It was also pointed out that an appropriate compromise should be the search for numerical indicators of road roughness to describe the profile and correlation with the vibration response of the vehicle, human body and perceived driving quality. Excessively long exposure to the vibrations of the defined intensity also leads to deterioration of the health of the vehicle users [8].

While analyzing the data received with the quarter car model used to determine the IRI, the authors of the article paid attention to the vibration of the wheel, as a result of the input and change of its position in the vertical direction but also, which is important in this approach, in the longitudinal direction [26]. Due to the specific structure of the car suspension, the longitudinal direction is not more susceptible to small inputs than the vertical direction (displacement occurs when driving through an irregularity). As a consequence, while maintaining a constant angular wheel velocity (vehicle speed), any force from the road roughness will result in acceleration of the body of the vehicle both longitudinally and vertically.

Temporary increases in acceleration can be used to determine the diagnostic parameter concerning the condition of the road surface under normal operating conditions. The presented method does not require the use of specialized measuring equipment in the form of a scanner and profilometer.

1.2. Objective of the Paper

To sum up the above considerations, the research on the method of identifying the state of the road's surface unevenness is still valid in this respect. Not only are the measuring procedures and techniques that allow the determination of IRI according to ISO 8606 being improved, but also alternative methods are being developed. These methods make it possible to determine the road surface unevenness using commonly available multiaxial acceleration sensors or devices that have such sensors built in, e.g., smartphones. A significant problem to be solved in all alternative methods of measurement is how to obtain a valuable signal of road roughness from the measuring noise of vertical acceleration of the car body. In this study, an algorithm for identifying the signal of longitudinal acceleration of the car body using its transformation to the frequency domain has been developed, which allows for the determination of the acceleration value at the dominant frequency, which enables the correct classification of the road surface condition as good. In this way it is possible to classify whether a car is driving on a road with good road surface. Such a classification is very important when, for example, you want to carry out diagnostics of the chassis, suspension or drive system of a vehicle in road conditions. The description of such diagnostics in real road conditions is the subject of many authors' studies [27–29]. Such a method will allow one to determine the measuring window for the vertical acceleration signal of the diagnosed vehicle with good road surface condition. The review of recent studies proves that in the further development of this methodology, the smartphone equipped with a multiaxial acceleration sensor may be an independent measuring device, as it can effectively capture vehicle vibrations. However, the key question is as follows. How to carry out the measurement, where to place the smartphone in the car body and how to select its attachment point? At the same time, of great importance, it is necessary to have a representative threshold value of the road surface condition classifier, obtained using much more accurate measuring equipment and from different vehicles. The above is necessary so that the existing measurement noise for the vertical axis acceleration signal is acceptable for the designated vertical acceleration measuring window. The classifier determined in the work, by analyzing several vehicles and different road surfaces, including laboratory tests, shows a threshold value below 0.02 m/s^2.

2. Identification of Periodic Vibrations of a Passenger Car Body

As a result of transport infrastructure activities and atmospheric conditions, road surface is subject to a more intensive wear. Road test sections selected by the authors of the study are part of roads intensively used by the transport industry.

For the purposes of this paper, in terms of the condition of the roadway surface, it is defined as: bituminous surface A (Figure 2a) without visible damage to the surface, bituminous surface B (Figure 2b) with visible cracks and a few defects in the surface, bituminous surface C (Figure 2c) with significant defects and poor standard of pavement with cracks and laterally uneven surface (folds).

Figure 2. The example of the road surface classified in the paper as: (**a**) A good, (**b**) B slightly damaged, (**c**) C bad.

The following parameters for road surface defects were assumed in the article: for the road B they did not exceed 0.005 m in width and 0.001 m in depth. On surface C there were significant irregularities and cavities exceeding 0.015 m in width and 0.001 to 0.005 m in depth.

2.1. Methodology

For the vehicle vibration analysis, a commonly used typical dual-mass model, referred to in the literature as the "quarter car model" (Figure 3), was employed [29]. For road condition identification tests used authors measurement platform on name PAAF (Power Acceleration And Force), the authors used several class C vehicles equipped with various types of McPherson suspensions such as: VW Passat B5, Citroen C5, Opel Vectra C. These vehicles were specified S1, S2, S3, respectively.
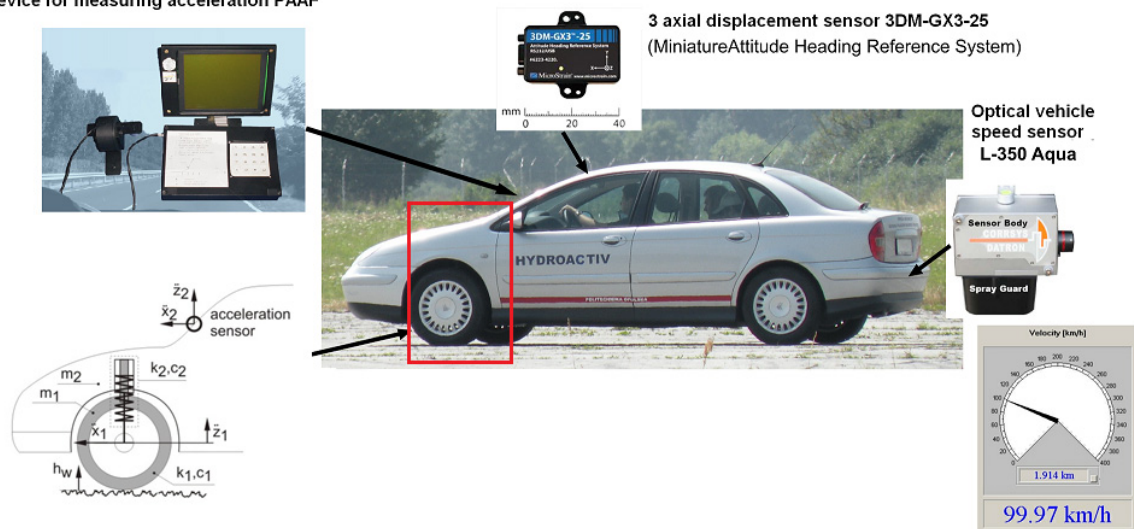
Figure 3. Dynamic system in the form of the quarter car model, where: m_1—unsprung mass, m_2—sprung mass, k_n—stiffness of mass n, c_n—damping coefficient of mass n, h_w—height of road surface roughness.

The model is made of sprung mass (m_2), unsprung mass (m_1) and elements connecting masses with elastic and damping properties (k, c). The mass' vibrations depend on their mechanical structure construction and excitation source. The increase in the wheel's vibrations has its origins in different factors such as: the road roughness, the homogeneity of tire and the wheel unbalance.

To identify periodic vibrations, selected signal analysis methods in the paper were used:

- in the time domain, the autocorrelation function $R_x(t)$,
- in the time and frequency domain—short term Fourier Transform (STFT),
- statistical—distribution of values in the sample (histogram).

As shown in Figure 4, the proposed system consists of two systems for measuring vehicle movement parameters. The first is a three-axial acceleration sensor mounted inside the vehicle on the windshield.
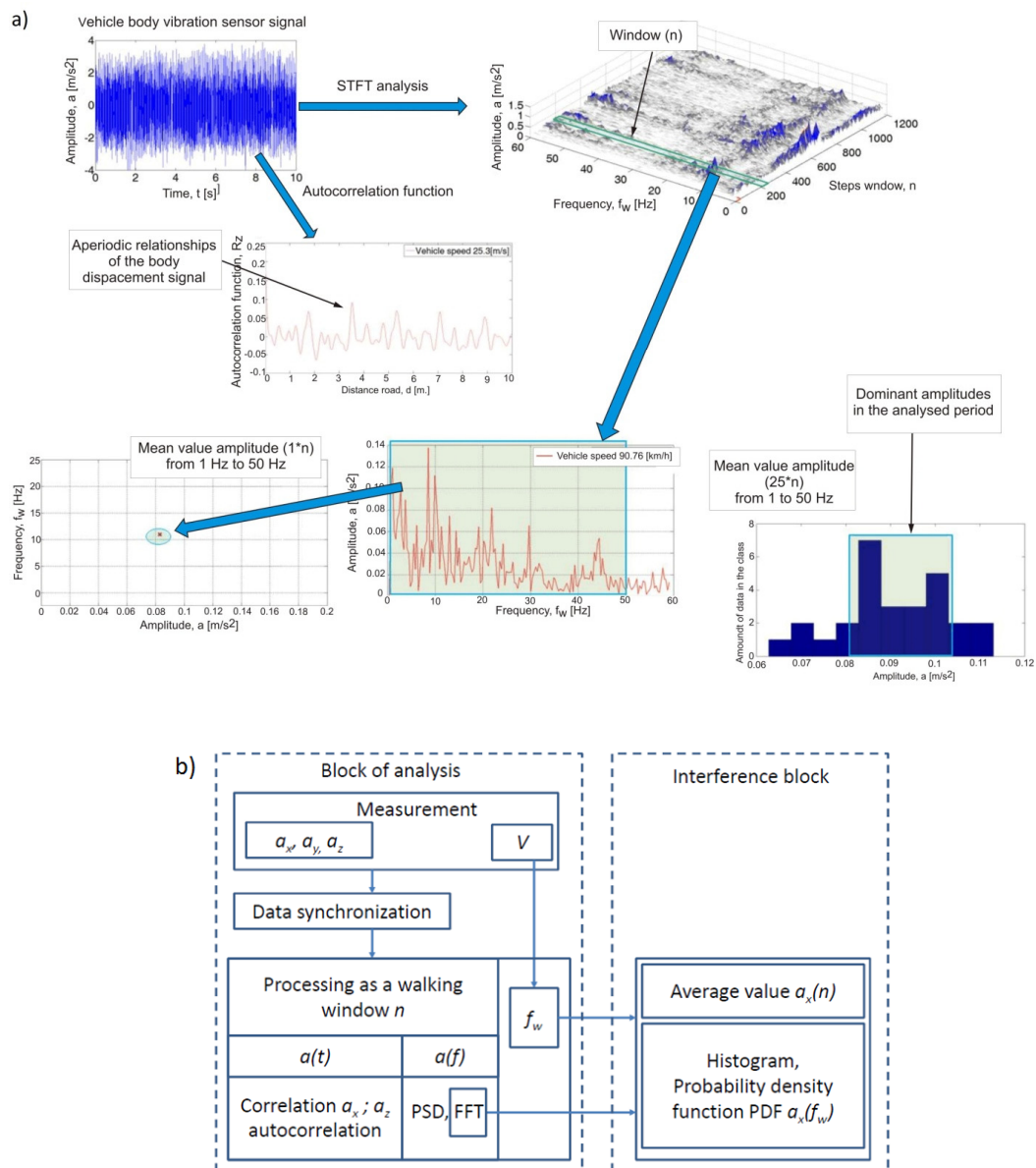
Figure 4. Diagram of processing data (**a**) and structure of measurement data analysis (**b**), where: a_x, a_y, a_z—body linear accelerations (in x, y, z direction), *V*—vehicle linear speed, *a*(t)—acceleration analyzed in the time domain, *a*(f)—acceleration analysis in the frequency domain, f_w—calculated wheel rotation frequency, $a_x(n)$—average value of the acceleration spectrum in the x direction for the adopted frequency range (n), $a_x(f_w)$—peak value of the acceleration spectrum in the x direction in the range of the wheel rotation frequency (f_w). STFT: short term Fourier Transform.

The second measuring system is used to determine the linear speed of the vehicle V. Based on the known vehicle speed, the wheel rotation frequency f_w is determined for the assumed tire size.

Data recorded from the acceleration sensor and the speed measuring system were synchronized. This is due to the difference in sampling frequency of the measuring systems used.

For mathematical analysis of the recorded signals, an application developed in the Matlab calculation package was used. The developed algorithms for data analysis were based on methods of signal analysis in the time domain $a(t)$ and frequency $a(f)$. The obtained results were further analyzed to relate the vibration spectrum with the road conditions. In this way, a description of the concentration level (dispersion) of the amplitude values in the spectrum of the analyzed signal from the acceleration sensor was obtained. The acceleration signal in the vertical as well as longitudinal direction was subjected to statistical analysis in the frequency range, which were determined in an experimental manner by the authors of the article [30].

2.2. Measuring System

The applied measurement system (Figure 5) enables the registration of kinematic and dynamic parameters of the car, which are recorded with the author's measuring platform "Road Test Application". The measurement devices include the multi-axial X, Y, Z acceleration sensor type 3DM-GX3-25 (sensor's specifications in Table 2), the head for non-contact measurement of body speed L-350 AQUA (sensor's specifications in Table 3), a series of analog tracks registered directly from sensors and digitally recorded from the on-board data transmission network. To synchronize the signal from the acceleration sensor and the vehicle speed sensor head, a proprietary application developed in the Matlab calculation package was used, where data from different measurement tracks are synchronized by the trigger of the measurement module, and then, after the integration of the acceleration signal, it is compared with the vehicle speed signal from the Optical Sensor Datron L-350 on the basis of the Kalman filter. The sampling frequency of the acceleration sensor was 866 Hz and the speed sensor sampling frequency was 20 Hz for comparison.
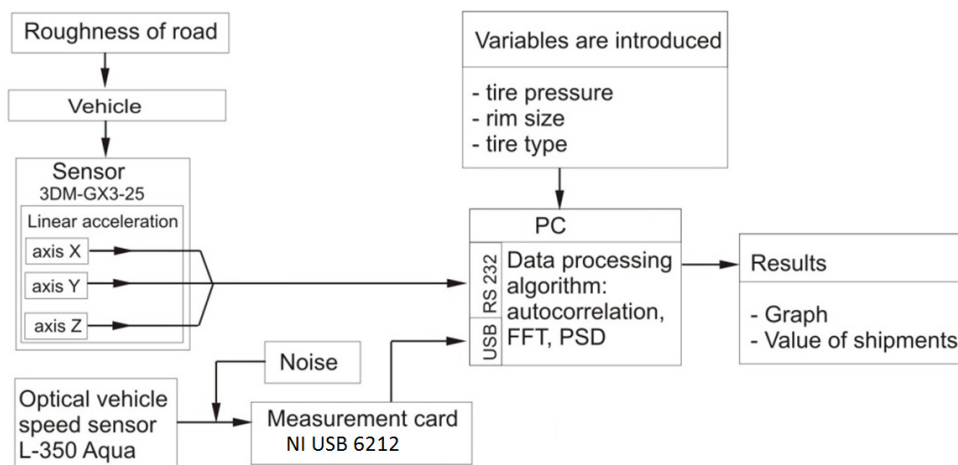
Figure 5. Block diagram of the measurement system. PSD: Spectral Power Density; FFT: Fast Fourier Transform.

Table 2. Acceleration sensor type 3DM-GX3-25 specifications.

Measurement range	+/−5 g
Non-linearity	±0.1% fs
In-run bias stability	±0.04 mg
Initial bias error	±0.002 g
Scale factor stability	±0.05%
Noise density	80 µg/$\sqrt{\text{Hz}}$
Data output rate	1000 Hz

Table 3. Datron L-350 Aqua specifications.

Speed range	0.3 . . . 250 kph
Distance resolution	Mm
Distance measurement deviation	<±0.1%
Speed linearity	<±0.2%
Working range linearity	<±0.2%

Vibration measurements of unsprung m1 and sprung mass m2 (Figure 3) were carried out for selected speeds in the range from 50 km/h to 110 km/h. The set longitudinal velocity of the vehicle was maintained for selected measuring sections for a period of 5 to 10 s. The selection of the time window period for the analyzed signal was determined based on the Pareto inference method. This issue has been described by the authors in another study [31].

3. Measurement Signal Analysis

3.1. Statistical Parameter Vibration

In order to determine the periodic vibrations of the body, the correlation function was proposed. These functions belong to the classic methods of analysis of deterministic signals disturbed by random noise [9,31]. To determine the periodicity of the analyzed signal in relation to time t, the autocorrelation function $R_{xx}(\tau)$, described by Equation (2), is used to identify the periodicities hidden in the noise of the analyzed acceleration of the body. It allows to determine the time consistency between adjacent fragments of the analyzed process (signal), shifted by different time values (t) and ($t + \tau$) [9]. By measuring the amplitude in two moments, separated by a delay (τ), and multiplying the obtained values and averaging them after the recording time, statistical information about the signal periodicity was obtained.

$$R_{xx}(\tau) = \lim_{T \to \infty} \frac{1}{T} \int_0^T x(t)x(t + \tau)dt \qquad (2)$$

where: τ is the time shift relative to time t, $R_{xx}(\tau)$- autocorrelation function.

In the case of a completely random signal (Figure 6), only for ($t = 0$) or close to (0) the value is normalized to unity and takes large values while the product of $x(t)$ $x(t + \tau)$ takes small values. For a signal with periodic components, a large shift (t), equal to half of the period, is needed to induce a significant change $R_{xx}(t)$. Values of autocorrelation function result from the superposition of the determined part of the process (containing, e.g., diagnostic information) and the stochastic part resulting from disturbances from other processes or measurement disturbances. This makes it possible to determine the share of the signal associated with the random disturbance in the total energy. Examples of the autocorrelation function graph obtained as a result of analysis of the data received during the road tests for the car body acceleration signal, are shown in Figure 6. This way it is possible to determine the rotational speed of the wheel by this method.
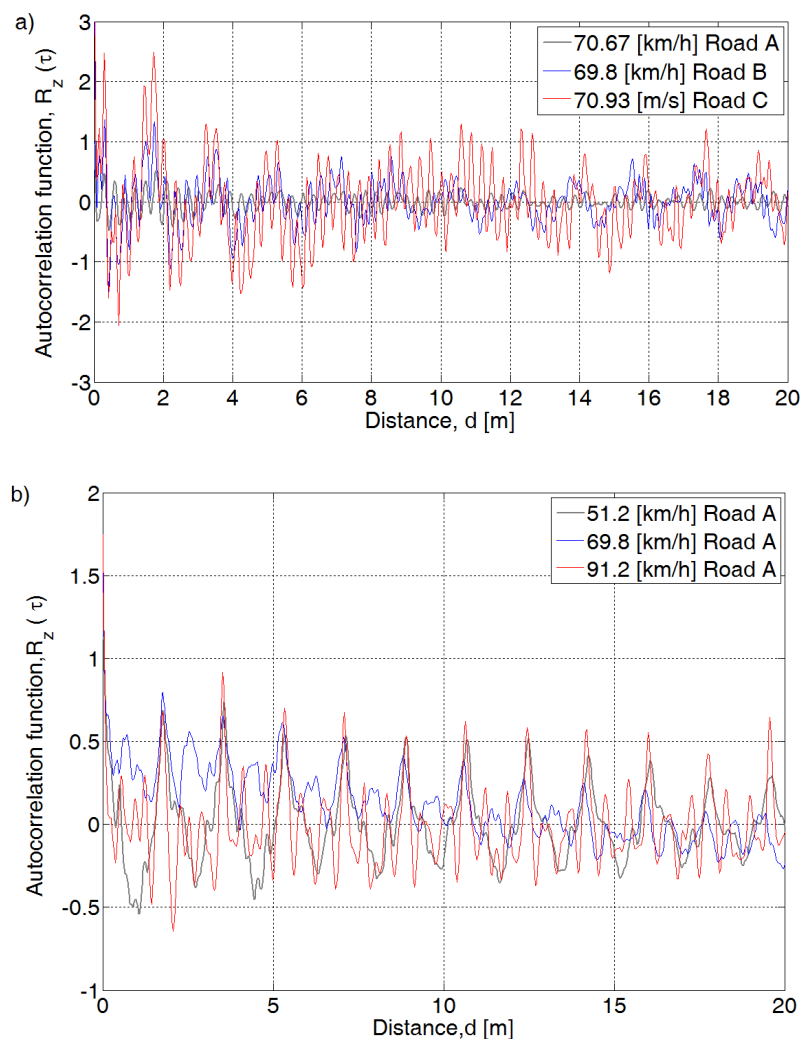
Figure 6. Graphs of the autocorrelation function of the body acceleration signal, for selected vehicle speeds different surfaces A, B, C for constant speed (**a**), and different speed (**b**) for road A.

Both for the vehicle speed and for different road surfaces, significant differences in the waveform over time can be seen. However, only on road surface A is the auto correlation repeated and oscillates close to zero, referring at the same time to the length of the travelled distance, as shown in Figure 6a. Therefore, for the tested road surface, it was checked whether this regularity occurs for different vehicle speeds, as shown in Figure 6b. In this range, no interference in the autocorrelation function was noticed. The harmonics of the autocorrelation function depend on the distance travelled and not on time, which overlap and oscillate around zero.

3.2. Data Analysis

To determine the frequency components of the recorded sinusoidal signal from the acceleration sensor for local signal segments changing in time, a Short-Time Fourier transform (STFT) was used. The STFT function describes Equation (3). This results in an integrated continuous function in the frequency domain f in the range from $-\infty$ to $+\infty$. (a), which allows one to determine the spectrum of the tested signal, its harmonic components and the level of their amplitudes.

$$X(f) = \int_{-\infty}^{+\infty} x(t)e^{-j2\pi ft}dt \qquad (3)$$

where: $X(f)$ is the frequency spectrum and $x(t)$ is the time function analyzed.

The signal spectrum contains harmonics, which are the result of excitation from many components of the car. An example of the spectrum classification for the recorded signal is shown in Figure 7. By analyzing the signal in specific frequency ranges, information about their source can be obtained. The occurring wheel malfunction (unbalance) will then be seen as the dominant amplitude in the wheel rotation frequency range. The band of occurrence of forces from the wheel in this area is visible in Figure 8.
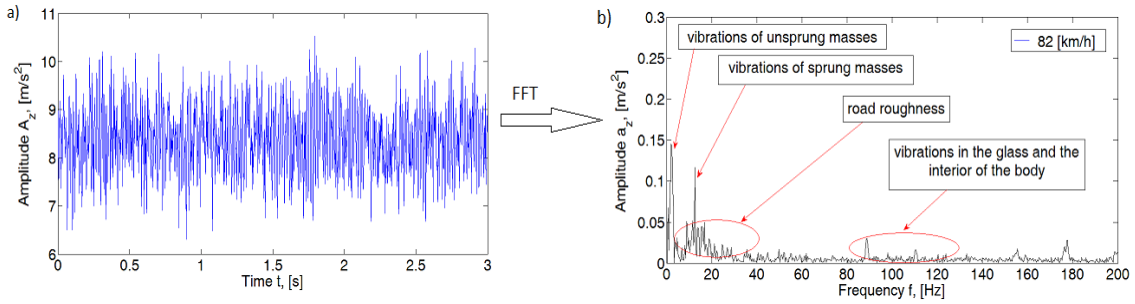
Figure 7. An example of acceleration signal processing (**a**), the effect of using Fourier transform to move from time domain to frequency domain (**b**).
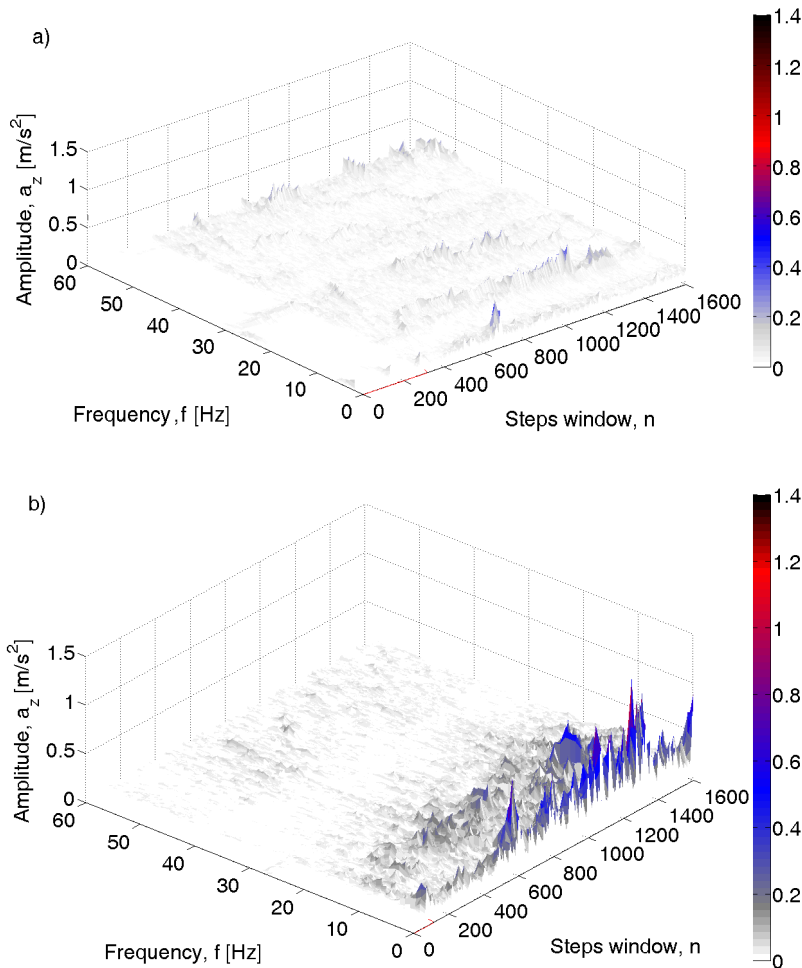
Figure 8. *Cont.*
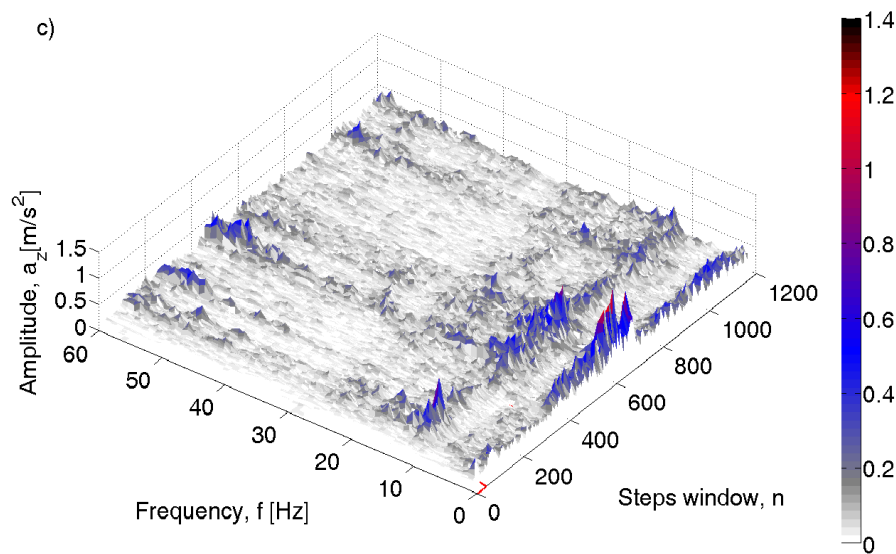
Figure 8. STFT spectrum of the car body acceleration signal in the vertical direction for the: (**a**) road surface A, (**b**) road surface B, (**c**) road surface C.

The use of Fourier transform allows obtaining information about the change in the spectrum of the analyzed signal, at certain parameters of the measurement window or frequency [32]. These issues are described in the publication [33,34]. Observing the pattern of the signal acceleration spectrum, its properties in the time and frequency domain, the primary and secondary frequencies can be identified. Selected results for bituminous road surfaces A, B and C are presented in Figure 8.

In the car body vibration spectrum for the road surface A the dominant amplitudes corresponding to the driving frequency of angular velocity of wheels are visible. The amplitudes for the first harmonic range from 0.07 m/s^2 to 0.25 m/s^2, depending on the linear speed of the car. For a passenger car moving at a speed greater than 40 km/h, for frequencies from 1 Hz to 5 Hz, amplitudes up to 0.12 m/s^2 are shown. For the frequency from 5 Hz up to the limit corresponding to the frequency of wheel rotation, the vibration amplitude of the car body is damped [28,31]. This phenomenon was found for all vehicles tested on road A. The amplitude of white noise interference does not exceed 0.05 m/s^2.

The roughness of the road surface B and C causes an increase in the amplitude of body vibrations in the vertical direction (a$_z$) in the frequency band from 1 Hz to 30 Hz, as shown in Figure 8b,c. Unlike the spectrum obtained for the road A, the amplitudes corresponding to the angular velocity of the car's wheels are not visible. This is related to the occurrence of significant unevenness of the road surface. The effect is a visible increase in background amplitudes in the frequency range up to 60 Hz from 0.02 m/s^2 for road surface A, up to 0.12 m/s^2 for road surface B and 0.18 m/s^2 for road surface C. In the obtained spectrograms local increases in amplitudes are also visible, which indicate significant unevenness and defects of the road surface.

In the amplitude spectra obtained for the road tests, there are also multiple increases in the body vibration amplitude along both the axis Y and Z, but attention was paid to the accelerations for the longitudinal axis (x axis), for tests carried out on road surfaces B and C as compared to road A.

The values of the vehicle body acceleration amplitude for the Z and Y axes are the result of both forced road roughness and the running gear. As it results from the kinematics of the suspension system, it shows the greatest susceptibility to excitations resulting from road unevenness in the vertical direction. The task of the applied elastic damping elements is then to minimize these inputs. As a consequence, vibrations in the vertical direction are the results of input from the road unevenness and dynamic forces resulting from the operation of the suspension system components. The stabilizing elements used in vehicles, on the other hand, limit the lateral movement (Y axis) of the body structure. However, as noted other studies [4,30], worn or unwashed elements of the vehicle chassis and suspension may cause additional exciting forces. Due to the limitation of the displacement of the sprung mass along

the longitudinal axis X, we mention the influence of the poor technical condition of the suspension elements (e.g., unbalance of the tire wheel), which does not significantly change the amplitude value due to road unevenness. Thus, the analysis of the longitudinal axis (x axis) can be a supplement to the analysis of the components of vehicle body acceleration in order to identify road unevenness.

The visible dominant amplitudes for speeds from 90 km/h to 92 km/h occur in the frequency range from 5 Hz to 25 Hz (Figures 9–11) for test surface conditions A, B and C and according to the diagram shown in Figure 4 (look the marked green box).
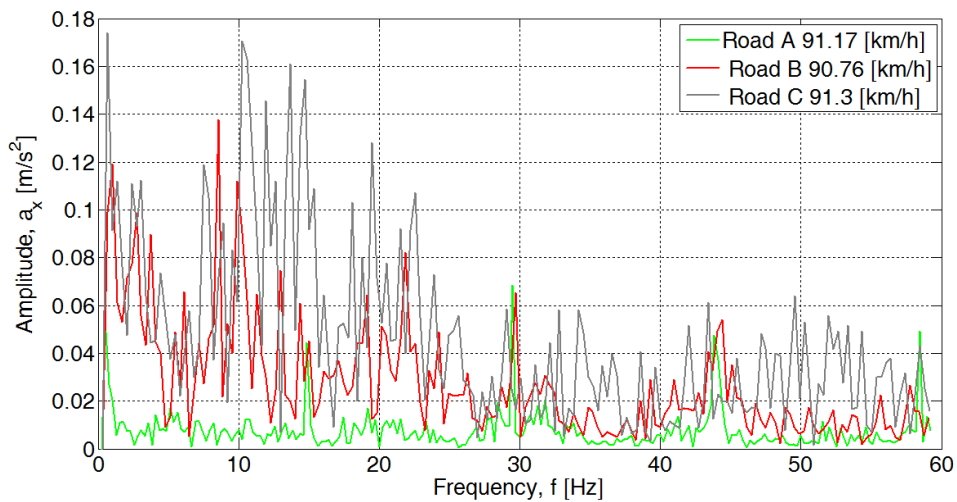
Figure 9. Amplitude of the body accelerations in the longitudinal direction for a selected random window for a given speed (x axis), for test surface conditions A, B and C.
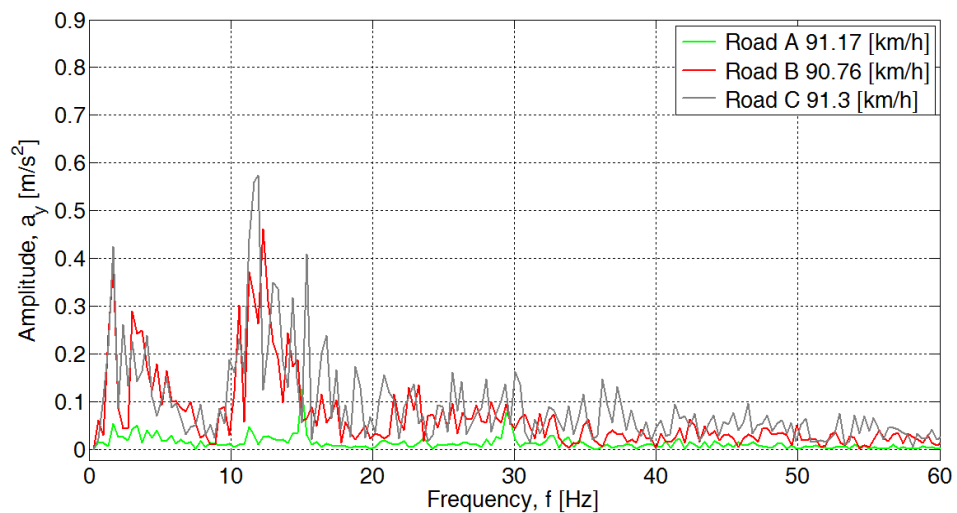
Figure 10. Amplitude of the body accelerations in the transverse direction for a selected random window for a given speed (y axis), for test surface conditions A, B and C.
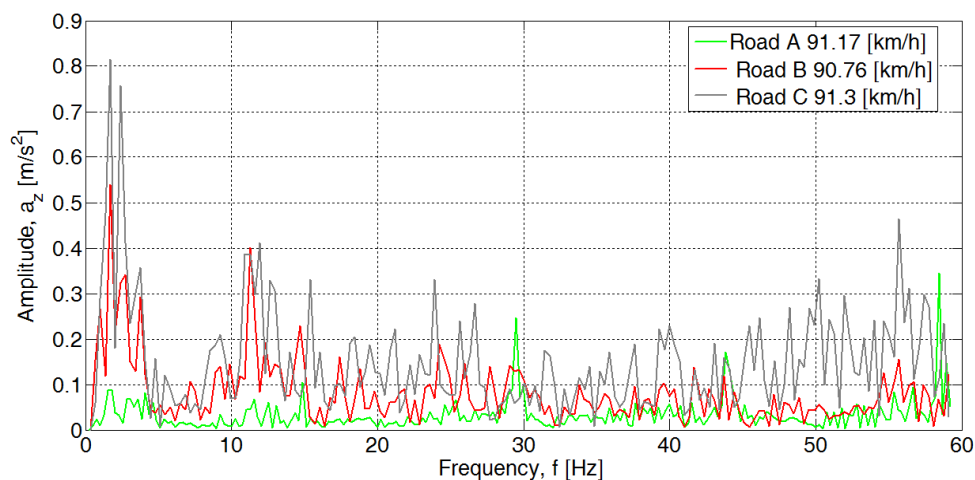
Figure 11. Amplitude of the body accelerations in the longitudinal direction for a selected random window for a given speed (z axis), for test surface conditions A, B and C.

In the longitudinal direction (Figure 9), a significant increase in the average amplitude value for the road surface B (0.02731 m/s^2) and C (0.04573 m/s^2) in comparison to the road surface A (0.007627 m/s^2) is noticeable (Table 4). For the road surface A, the maximum value of the acceleration amplitude in the frequency around 15 Hz, corresponding to the basic frequency of wheel rotation, is 0.04 m/s^2. Similarly, in the vertical direction (axis Z) and horizontal transverse (axis Y), despite the vibration damping by the tire and suspension elements, an increase in the mean value of the acceleration amplitudes for road surfaces B and C, compared to the surface A, is visible and the waveforms are very similar to each other. Table 4 shows the mean values and standard deviations for the body acceleration amplitude spectra shown in Figures 9–11. In the case of the measurement axes under consideration, the standard deviation used in statistics, as a measure of the scatter of individual measurement values around the mean value, reaches the lowest values for the ax axis. On the other hand, the standard deviation for both road surfaces B and C increases two to three times.

Table 4. Example of statistical values for amplitude spectra of the body acceleration for different road surfaces. Statistical values for amplitude spectra of the body acceleration for different road surfaces.

Surface	a_x		a_y		a_z	
	Mean Value (m/s^2)	Standard Deviation	Mean Value (m/s^2)	Standard Deviation	Mean Value (m/s^2)	Standard Deviation
A	0.0076	0.008	0.006	0.009	0.033	0.035
B	0.027	0.024	0.034	0.055	0.081	0.072
C	0.045	0.037	0.053	0.066	0.15	0.11

Unevenness and damages of road surface B and C in the longitudinal direction cause a 3.5 and 6-fold increase in the mean amplitude value in relation to the mean amplitude value of body accelerations on the damage-free road surface A. In the vertical direction, however, much smaller increases in the mean amplitude value for the road B and C in relation to the road A were found. This proves that the condition of the road surface has a significant impact on the acceleration amplitude value of the body especially in case of longitudinal acceleration. Therefore, the measurement of body acceleration in the longitudinal direction may be the measure of interference caused by road roughness [29,35].

### 3.3. Assessment of the Condition of the Pavement

The assessment of the condition of the road surface can be made on the basis of the acceleration signal of the car body with particular attention paid to the longitudinal acceleration of a passenger car under real traffic conditions. For this purpose, the average value of the bandwidth acceleration signal of the longitudinal axis (x-axis) of the car body in the frequency range from 0 to 60 Hz for each walking time window of STFT function was used. The examples of results for several tested passenger cars S1, S2, S3 on the good condition road surface A are shown in Figure 12.
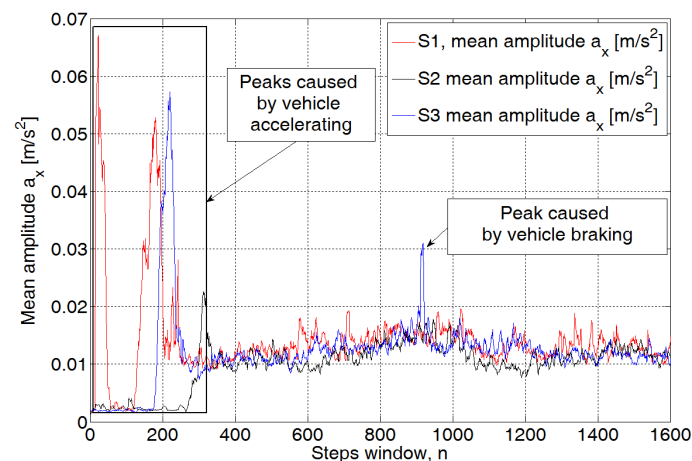
Figure 12. Average value of the passenger car body longitudinal acceleration signal during the test on road surface A.

The paper attempts to estimate the limit value of the longitudinal acceleration signal (a_x), which is equivalent to a good road surface. For further analysis of the acceleration of the body, sections were taken on which a constant speed was kept. The analyzed sections are marked with a gray box, which is shown in Figure 13. The tests were carried out for several test cars with the speed changing in the range from 50 km/h to 100 km/h. For selected sections driven at a constant speed (the red line inside grey boxes) on the road with a good road surface condition, an analysis was carried out of the average values of longitudinal acceleration a_x, which is indicated by the blue line in the figure below. The mean values for the analyzed vehicle speeds (wheel angular speed) are shown in Figure 13. The first section in Figure 12, included in windows 0 to 300, is not taken into account for testing. This is the distance needed to perform a shakedown ride and is not used in normal operation due to the acceleration of the vehicle.

For the sections with a constant linear speed of the car (Figure 14), ranges of mean longitudinal car accelerations were determined, which are from 0.011 m/s^2 to 0.017 m/s^2. In this way, it was determined that for the cars tested on the good road surface A, the range of the limit value of the car body acceleration in the longitudinal direction can be assumed to be 0.017 m/s^2. In this case, the mean value of the longitudinal acceleration of the body does not depend on the value of the angular velocity of the car (while maintaining the measuring window for 3 s), as shown in Figure 13 in brown. Similar results were obtained for the remaining test cars.
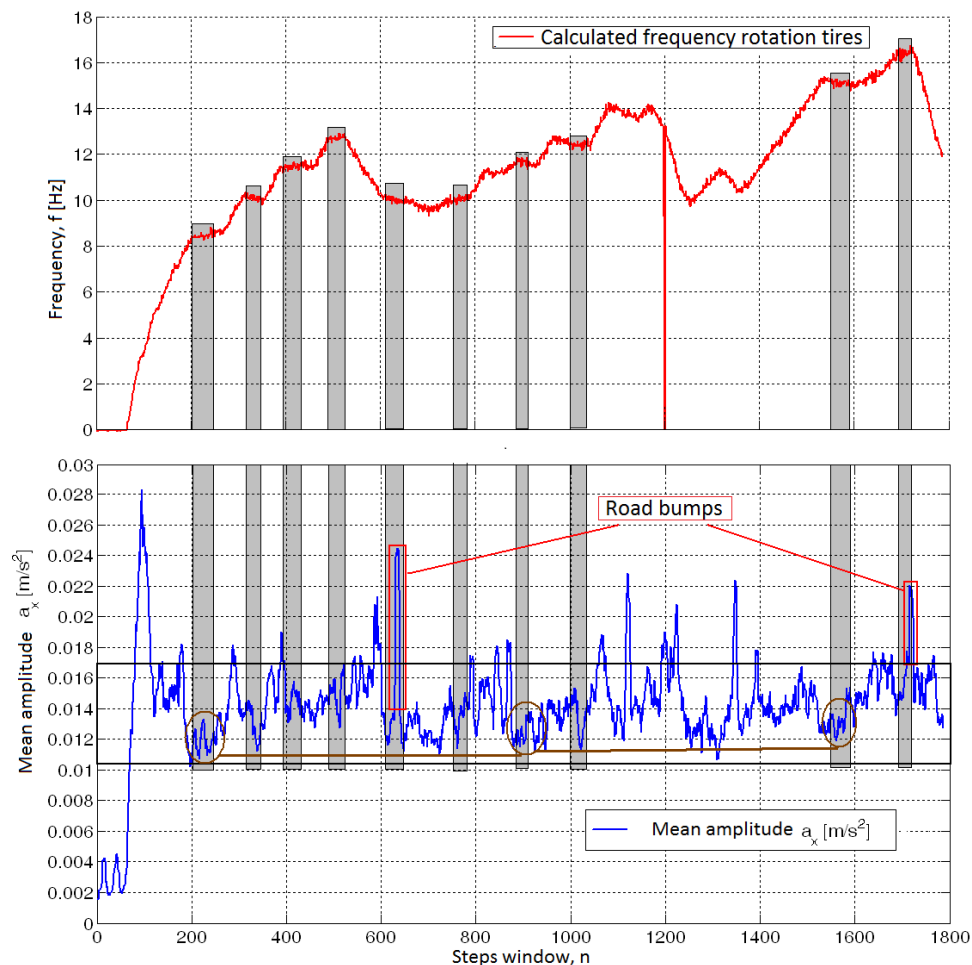
Figure 13. Mean value of signal for longitudinal axis (x-axis). Grey boxes point distances with the constant speed.

The sample values for the ranges under consideration were sorted and grouped into classes concerning the different variable of driving frequency. The classes were selected according to the sample size so that the information about the examined population (too small) and data transparency (too large) was not lost [33]. In this way, frequency distribution was obtained in the form of a histogram, which enabled the qualitative and quantitative evaluation of the pattern of the distribution of the results. The presence of two or more maxima means that the sample is heterogeneous and the variables show a more even distribution of values over the whole range. The information obtained about the quantitative affiliation of a variable to a given class may be used to determine the percentage of the whole population under consideration.

Below, in Figure 14, the probability distribution densities for different road surfaces are shown.
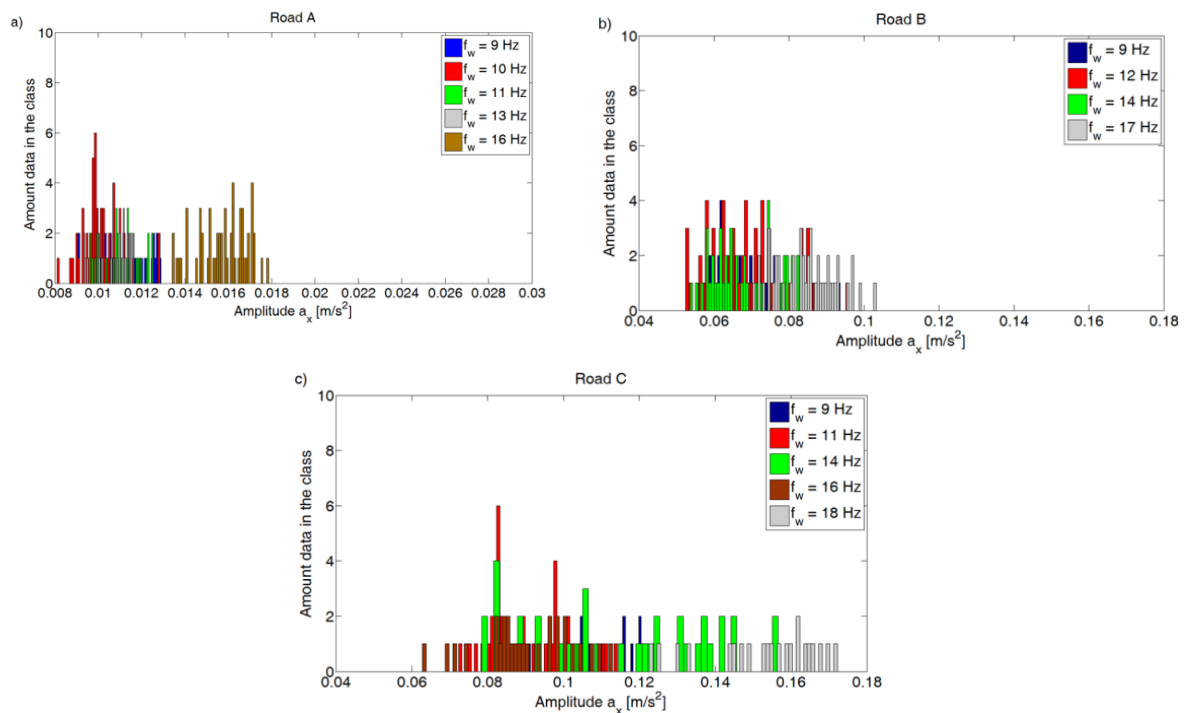
Figure 14. Histogram of variable a_x for road surface (**a**) good A, (**b**) slightly damaged B, (**c**) bad C.

In the histogram for the road surface A (Figure 14—green) it was observed that the distribution of amplitudes in the longitudinal direction for frequencies from 9 Hz to 16 Hz is in the range from 0.08 m/s^2 to 0.017 m/s^2. For frequencies: 10 Hz, 11 Hz and 13 Hz, the amplitude range is between 0.069 m/s^2 and 0.0125 m/s^2 and it takes a more even shape with the two distinct modes. For 16 Hz frequency, a maximum shift towards the higher acceleration amplitude is visible and it is 0.0165 m/s^2. The effect of the car's linear speed on the average acceleration of the body in the longitudinal direction, is also visible at 16 Hz for other types of road surfaces.

In the case of the roadway surface B, for the frequency range of wheel rotation from 9 Hz to 15 Hz (Figure 14—blue) the dominant amplitudes are in the range from 0.069 m/s^2 to 0.0754 m/s^2. An increase in the driving frequency of wheel rotation above this value also causes a shift in the maximum. The difference in amplitude values visible at 17 Hz is 0.0983 m/s^2. Below this value, all the dominant car body vibration modes are within this range, which indicates that there is no significant effect of the vehicle speed on the amplitude value.

For the roadway surface **C,** there is no visible concentration of dominant mode values and they are significantly lower (Figure 14—red color). At the same time, an increase in the driving frequency of the wheel rotation, for example to 16 Hz, causes the mode value to be lower than for 9 Hz. An increase in the amplitude values for 14 Hz and 16 Hz is visible in relation to the results obtained for road B. There is also a significant increase in the amplitude values (one row higher) in relation to road A.

By analyzing the above graphs and mode values, information was obtained on the values of dominant amplitudes for selected frequency ranges of the tire rolling along the road A, B and C. On this basis, the characteristics of longitudinal accelerations of the car body for a constant driving speed were developed as a function of the driving frequency of the tire rotation (Figure 15). Based on this, a limit value of acceleration of the car body in the direction of the longitudinal axis was adopted at the level of 0.02 m/s^2, below which the condition of the road surface was clearly defined as good and is marked in the drawing with a rectangular outline for the different vehicle speeds determined by the wheel rotation frequency f_w.
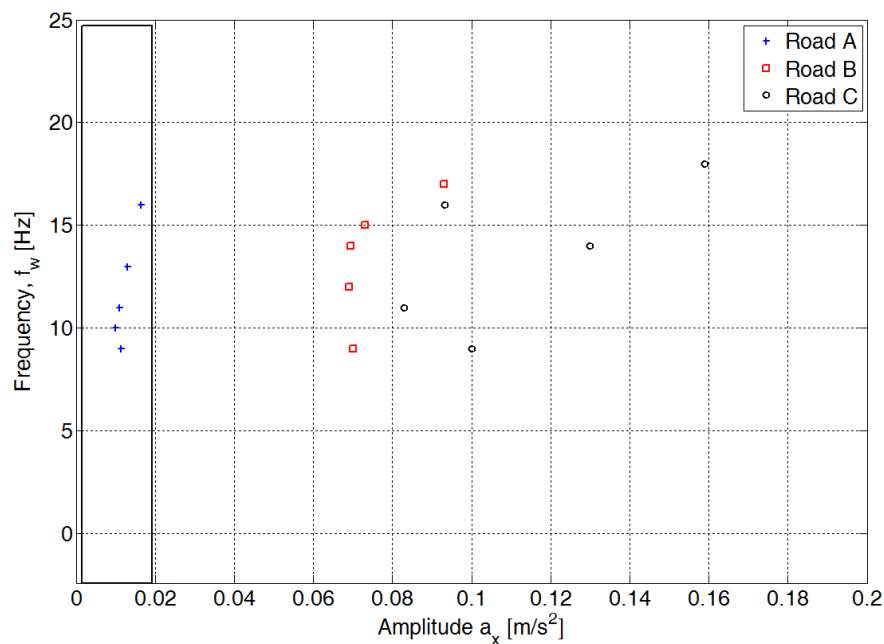
Figure 15. Limit value of longitudinal acceleration of the car body for which the condition of the road surface is classified as good.

4. Conclusions

As a result of the application of selected methods of vehicle vibration analysis based on acceleration signal in the time and frequency domain, it was found that apart from random properties, the recorded acceleration signal also shows deterministic properties. This conclusion was based on the obtained autocorrelation function correlograms, where cyclic harmonics repeated at regular intervals were found.

The analysis of the signal by means of the Fourier transform, showed the dominant harmonic components in the range of driving frequency of the tire rotation (Figure 15). The road tests carried out for determining the state of the road surface on the basis of the acceleration signal of the car body showed that these vibrations can be the basis for conclusions about the state of the road surface.

As a result of the tests, it was found that the unevenness of the pavement (road in poor technical condition) has an impact on the longitudinal vibrations of the vehicle body. The obtained results show that the analysis of the mean value of the longitudinal axis spectrum is the basis for the assessment of the road surface condition. Contrary to vertical accelerations, longitudinal vibrations are not affected by additional forces caused by vertically moving suspension elements. As a result, additional exciting forces arise that can increase or decrease the amplitude of the car body.

Our results show that the value of longitudinal acceleration increases two-fold compared to the amplitude of the acceleration specified for good road surface condition. Based on the results of road tests, it was determined that this range is up to 0.02 m/s^2 for the longitudinal acceleration of the car body at a constant linear velocity.

The presentation with histograms of the car body acceleration allows one to draw correct conclusions as well as to visualize the condition of the road surface. Such an approach allows, with the application of signal processing methodology, to improve the choice of a road with good surface in autonomous systems of the car.

By performing a re-analysis in the assumed periods of time, it is possible to determine the progress of pavement degradation. This is the next step in the research work concerning the determination of the technical condition of the road surface.

The presented method of road surface condition assessment is an element of the further measurement procedure, which aims at identifying the malfunctions of the chassis and powertrain under real vehicle operation conditions. In order to improve the quality of conclusions, the authors

plan to use more advanced measurement methods, including Bayers' classifier or artificial neutral network (ANN) or fuzzy logic.

References

1. Karacocuk, G.; Höflinger, F.; Zhang, R.; Reindl, L.M.; Laufer, B.; Möller, K.; Röell, M.; Zdzieblik, D. Inertial sensor-based respiration analysis. *IEEE Trans. Instrum. Meas.* **2019**, *68*, 4268–4275. [CrossRef]

2. Nabavi, S.; Bhadra, S. A robust fusion method for motion artifacts reduction in photoplethysmography signal. *IEEE Trans. Instrum. Meas.* **2020**. [CrossRef]

3. Burdzik, R. Identification of structure and directional distribution of vibration transferred to car-body from road roughness. *J. Vibroengineering* **2014**, *16*, 324–333.

4. Prażnowski, K.; Mamala, J. Problems in assessing pneumatic tire unbalance of a passenger car determined with test road in normal conditions. SAE Technical Paper 2017-01-1805. *Noise Vib. Conf. Exhib.* **2017**. [CrossRef]

5. Sun, L. An overview of a unified theory of dynamics of vehicle–pavement interaction under moving and stochastic load. *J. Mod. Transp.* **2013**, *21*, 135–162. [CrossRef]

6. Levulytė, L.; Žuraulis, V.; Sokolovskij, E. The research of dynamic characteristics of a vehicle driving over road roughness. *Eksploat. Niezawodn. Maint. Reliab.* **2014**, *16*, 518–525.

7. Burdzik, R. Novel method for research on exposure to nonlinear vibration transferred by suspension of vehicle. *Int. J. Non-Linear Mech.* **2017**, *91*, 170–180. [CrossRef]

8. He, S.; Tang, T.; Ye, M.; Xu, E.; Deng, J.; Tang, R. A domain association hierarchical decomposition optimization method for cab vibration control of commercial vehicles. *Measurement* **2019**, *138*, 497–513. [CrossRef]

9. Múčka, P. Simulated road profiles according to ISO 8608 in vibration analysis. *J. Test. Eval.* **2018**, *46*, 20160265. [CrossRef]

10. Múčka, P.; Granlund, J. Comparison of longitudinal unevenness of old and repaired highway lanes. *J. Transp. Eng. ASCE* **2012**, *138*, 371–380. [CrossRef]

11. Gobbi, M.; Levi, F.; Mastinu, G. Multi-objective stochastic optimization of the suspension system of road vehicles. *J. Sound Vib.* **2006**, *298*, 1055–1072. [CrossRef]

12. Burdzik, R.; Konieczny, Ł.; Warczek, J.; Cioch, W. Adapted linear decimation procedures for TFR analysis of non-stationary vibration signals of vehicle suspensions. *Mech. Res. Commun.* **2017**, *82*, 29–35.

13. Byoung, S.K.; Chang, H.C.; Tae, K.L. *A Study on Radial Directional Natural Frequency and Damping Ratio in a Vehicle Tire*; Elsevier, Applied Acoustics: Amsterdam, Netherlands, 2007; Volume 68, pp. 538–556.

14. Harikrishnan, P.M.; Gopi, V.P. Vehicle vibration signal processing for road surface monitoring. *IEEE Sens. J.* **2017**, *17*, 5192–5197. [CrossRef]

15. Melcer, J. Dynamic Load on Pavement—Numerical Analysis. Scientific Journals of the Częstochowa University of Technology 2017, Construction series 23, 205–218. Available online: https://bud.pcz.pl/budownictwo-23 (accessed on 22 October 2020).

16. Coenen, T.B.J.; Golroo, A. A review on automated pavement distress detection methods. *Cogent Eng.* **2017**, *4*, 1374822. [CrossRef]

17. Chiculita, C.; Frangu, L. A low-cost car vibration acquisition system. In Proceedings of the 21st International Symposium/or Design and Technology in Electronic Packaging (SIITME), Brasov, 22–25 October 2015; IEEE: Oradea, Romania, 2015; pp. 281–285. [CrossRef]

18. Katicha, S.W.; El Khoury, J.; Flintsch, G.W. Assessing the effectiveness of probe vehicle acceleration measurements in estimating road roughness. *Int. J. Pavement Eng.* **2016**, *17*, 698–708. [CrossRef]

19. Douangphachanh, V.; Oneyama, H. A model for the estimation of road roughness condition from sensor data collected by android smartphones. *JJSCE SerD3 Infrastruct. Plan. Manag.* **2014**, *70*, I_103–I_111. [CrossRef]

20. Zang, K.; Shen, J.; Huang, H.; Wan, M.; Shi, J. Assessing and mapping of road surface roughness based on gps and accelerometer sensors on bicycle-mounted smartphones. *Sensors* **2018**, *18*, 914. [CrossRef]

21. Singh, G.; Bansal, D.; Sofat, S.; Aggarwal, N. Smart patrolling: An efficient road surface monitoring using smartphone sensors and crowdsourcing. *Pervasive Mob. Comput.* **2017**, *40*, 71–88. [CrossRef]

22. Du, R.; Qiu, G.; Gao, K.; Hu, L.; Liu, L. Abnormal road surface recognition based on smartphone acceleration sensor. *Sensors* **2020**, *20*, 451. [CrossRef]

23. Sayers, M.W. On the calculation of international roughness index from longitudinal road profile. *Transp. Res. Rec.* **1995**, *1501*, 1–12.

24. Kırbaş, U. IRI sensitivity to the influence of surface distress on flexible pavements. *Coatings* **2018**, *8*, 271. [CrossRef]

25. Pavementinteractive Roughness. Available online: http://www.pavementinteractive.org/roughness/ (accessed on 11 February 2018).

26. Pacejka, H.B. *Tire and Vehicle Dynamics*; Butterworth-Heinemann, Hardcover; Elsevier, Imprint: Amsterdam, The Netherlands, 2006; ISBN 97807500669184.

27. Brol, S.; Mamala, J. Application of spectral and wavelet analysis in power train system diagnostic. *SAE Tech. Pap.* **2010**, *01-0250*. [CrossRef]

28. Mamala, J.; Brol, S.; Jantos, J. The estimation of the engine power with use of an accelerometer. *SAE Tech. Pap.* **2010**, *01-0929*. [CrossRef]

29. Jantos, J.; Brol, S.; Mamala, J. Problems in assessing road vehicle drivability parameters determined with the aid of accelerometer. *SAE Trans. J. Passeng. Cars-Mech. Syst.* **2008**, *116*, 1318–1324.

30. Prażnowski, K.; Mamala, J. Application of bayes classifier to assess the state of unbalance wheel. Industrial measurements in machining. In *IMM 2019. Lecture Notes in Mechanical Engineering*; Springer: Berlin/Heidelberg, Germany, 2020. [CrossRef]

31. Bendat, J.S. *Nonlinear System Techniques and Applications*; John Wiley& Sons Inc.: New York, NY, USA, 1998.

32. Andria, G.; Savino, M.; Trott, A. FFT-based algorithms oriented to measurements on multifrequency signals. *Measurement* **1993**, *12*, 25–42. [CrossRef]

33. Bendat, J.S.; Piersol, A.G. *Random Data. Analysis and Measurement Procedures*; John Wiley& Sons Inc.: New York, NY, USA, 2010.

34. Chen, K.F.; Cao, X.; Li, Y.F. Sine wave fitting to short records initialized with the frequency retrieved from Hanning windowed FFT spectrum. *Measurement* **2009**, *42*, 127–135. [CrossRef]

35. Mamala, J.; Prażnowski, K. Classification of the road surface condition on the basis of vibrations of the sprung mass in a passenger car. *IOP Conf. Ser. Mater. Sci. Eng.* **2016**, *148*, 1–10. [CrossRef]

Publisher's Note: MDPI stays neutral with regard to jurisdictional claims in published maps and institutional affiliations.